Supplement of Atmos. Chem. Phys., 20, 6147–6158, 2020
https://doi.org/10.5194/acp-20-6147-2020-supplement

Atmospheric Chemistry and Physics
Open Access
EGU

Supplement of

Significant production of $ClNO_2$ and possible source of Cl_2 from N_2O_5 uptake at a suburban site in eastern China

Men Xia et al.

Correspondence to: Tao Wang (cetwang@polyu.edu.hk)

Table of Contents

Text S1: CIMS calibrations and data validation

S1.1. Dependence of the N_2O_5 sensitivity on RH

In the ion molecular reaction (IMR) chamber, the reagent ion I^- reacts with H_2O to form the iodide water cluster, $I^-(H_2O)$ which also reacts with N_2O_5 to produce $IN_2O_5^-$ (Kercher et al., 2009). Also, N_2O_5 may undergo hydrolysis in the sampling system. Thus, the sensitivity of N_2O_5 depends on the RH. In this study, the N_2O_5 signal was normalized to the $I(H_2O)^-$ signal (Hz 145) to account for the change of primary ions. During the field measurements, we monitored the RH at the indoor inlet of CIMS. When conducting calibrations, we tested the relationship between the normalized N_2O_5 sensitivity and RH (Fig. S5). A quadratic relationship in Fig. S5 ($y=-3.78\times10^{-9}x^2+1.69\times10^{-7}x+1.72\times10^{-5}$) was used to correct the RH effect on the ambient N_2O_5 data.

S1.2. Isotopic analysis of $ClNO_2$ and Cl_2

The $ClNO_2$ signals were recorded at mass 208 and 210 amu, representing $^{35}ClNO_2$ and $^{37}ClNO_2$, respectively. The relationship between the 208 and 210 signals was examined (Fig. S4). During ambient samplings, the slope of the Hz 210-Hz 208 plot was 0.3135 with $R^2=0.998$ (Fig. S4a). And the slope was 0.3154 with $R^2=0.999$ (Fig. S4a) during calibrations. The isotopic analysis was also performed for Cl_2. The correlations between mass 197 amu ($^{35}Cl^{35}Cl$) and 199 amu ($^{35}Cl^{37}Cl$) were excellent with $R^2=0.999$ for calibration data and $R^2=0.965$ for the ambient

data (Fig. S4b). The slope of the plot was 0.599 and 0.558 for the ambient data and calibration data, respectively, which is similar to previous studies (Liao et al., 2014). These results confirmed the identity of $ClNO_2$ and Cl_2 and indicated virtually no interference for $ClNO_2$ and negligible interference for Cl_2.

S1.3 Potential artifact of the inlet

When sampling ambient air, ambient particles gradually deposit on the inner wall of the sampling tubing. After a period of time, N_2O_5 in the ambient air reacts with the deposited particles, resulting in N_2O_5 loss and $ClNO_2$ formation. This inlet chemistry may cause underestimation of N_2O_5 and overestimation of $ClNO_2$. To minimize the interference from the sampling inlet, we adopted a virtual impactor design and a by-pass flow. The inlet design ensured that larger particles were mostly pumped through the by-pass flow. And the increased total flow (10 Lpm) reduced the residence time of N_2O_5 on the inlet. The sampling line was replaced daily by a cleansed one just before dusk to achieve minimum artifact on nighttime measurements.

We quantified the percentage of N_2O_5 loss and $ClNO_2$ formation in the inlet under different RH. After sampling for 24 hours, the used sampling line was taken indoor and connected to a zero-air generator with a flow rate of 10 Lpm. Then, we injected N_2O_5 at one end of the sampling line and measured the outflow at the other end in CIMS. The injected mixing ratios of N_2O_5 was determined by introducing N_2O_5 directly into the CIMS without passing the sampling line. The CIMS only inhaled ~1.5 Lpm airflow while the remaining ~8.5 Lpm airflow was discarded as a by-pass flow. The percentage of N_2O_5 loss and $ClNO_2$ yield ($ClNO_2$ production divided by N_2O_5 loss) increased with RH. When RH = 40 %, the N_2O_5 loss was 16.6 %. Thus, we assumed that the inlet artifact caused up to 16.6 % uncertainties for the ambient measurement of N_2O_5 and $ClNO_2$. 40 % RH was selected because the average RH recorded at the inlet of the CIMS was 40 % during the whole campaign. Cl_2 formation on the sampling tube was negligible in the wall-loss testing.

S1.4. Details of Cl_2 calibration

The Cl_2 standard was generated from a permeation tube heated to 40 ℃ and flushed by ultrapure nitrogen gas (20 sccm) and then diluted in humidified zero air (6 SLPM). During the field campaign, Cl_2 from the permeation tube was introduced into a KI solution (2% wt) for 1 hour. The permeation rate of Cl_2 (380 ± 20 ng/min) was calculated from the I_3^- concentration in the KI solution which was measured by ultraviolet–visible spectrophotometry at 351 nm.

Table S1. Measuring technique, detection limit and time resolution of the instruments in the field study. Detection limits were determined by 3σ of the noise level in 10 min.

Measured species	Techniques	Detection limits	Time resolution
N_2O_5, $ClNO_2$, Cl_2, HOCl, BrCl	Q-CIMS	2~7 pptv	10 s
NO, NO_2	Chemiluminescence with photolytic converter	0.06 ppbv	1 min
NO_y	Chemiluminescence with MoO converter	0.1 ppbv	1 min
CO	Infrared photometry	4 ppbv	1 min

SO_2	Pulsed ultraviolet fluorescence	0.1 ppbv	1 min
O_3	Ultraviolet photometry	0.5 ppbv	1 min
HONO	LOPAP	5 pptv	1 min
HNO_3	ion chromatography	0.05 ppbv	1 hour
$PM_{2.5}$	TEOM	1 $\mu g/m^3$	1 min
NH_4^+, Cl^-, NO_3^-, SO_4^{2-}	ToF-ACSM	0.01~0.06 $\mu g/m^3$	10 min
jNO_2	Filter radiometer	4×10^{-5} s^{-1}	10 s
VOCs	PTR-TOF-MS	10 pptv	10 min

Table S2. Summary of $\gamma(N_2O_5)$, $\varphi(ClNO_2)$, and $\varphi(Cl_2)$ (where applicable) in the selected 15 nighttime cases.

plume	start	end	$\gamma(N_2O_5)$	$\varphi(ClNO_2)$	$\varphi(Cl_2)$
1	4/12/18 2:10	4/12/18 3:00	0.0043	0.885	0.037±0.004
2	4/12/18 3:10	4/12/18 3:40	0.0068	0.716	0.021±0.003
3	4/12/18 21:40	4/13/18 0:40	0.0061	0.853	0.036±0.004
4	4/16/18 19:50	4/16/18 20:30	0.0031	0.378	0.013±0.000
5	4/16/18 20:40	4/16/18 21:20	0.0033	0.541	0.012±0.001
6	4/17/18 22:20	4/17/18 23:40	0.0058	0.521	0.010±0.001
7	4/18/18 3:00	4/18/18 3:50	0.0135	0.483	-
8	4/18/18 4:10	4/18/18 4:40	0.0139	0.187	-
9	4/19/18 0:00	4/19/18 0:40	0.0055	0.280	0.014±0.001
10	4/19/18 0:40	4/19/18 1:40	0.0041	0.523	0.018±0.002
11	4/19/18 2:00	4/19/18 3:00	0.0091	0.769	0.006±0.001
12	4/20/18 1:00	4/20/18 2:00	0.0084	0.641	0.013±0.001
13	4/20/18 2:10	4/20/18 2:50	0.0074	0.647	0.013±0.000
14	4/26/18 1:20	4/26/18 2:00	0.0136	0.468	0.006±0.001
15	4/26/18 2:30	4/26/18 3:20	0.0125	0.533	0.013±0.002
Average ± standard deviation			0.008±0.004	0.562±0.197	0.016±0.010

Table S3. Uncertainty analysis of the measured and deducted parameters. The uncertainty of Cl^-, NO_3^-, SO_4^{2-}, and S_a were referred to previous studies (Tham et al., 2016;Tham et al., 2018).

Parameter	sources of uncertainty (if any)			Propagated error	Reference
N_2O_5, $ClNO_2$	Signal precision 3.0 %	calibration 8.3 %	inlet interference 16.6 %	18.8 %	This study
Cl_2	Signal precision 3.0 %	calibration 10.0 %	inlet interference neglected	10.4 %	This study
$[Cl^-]$, $[NO_3^-]$, $[H_2O]$	ACSM 10.0 %		E-AIM model 15 % (assumed)	18.0 %	This study
$[H^+]$	Cl^-, NO_3^-, SO_4^{2-}, NH_4^+ 10 %, 10 %, 10 %, 10 %		E-AIM model 15 % (assumed)	25.0 %	This study
$\gamma(N_2O_5)$	N_2O_5, $ClNO_2$	NO_3^-	S_a	34.2 %	This study

	18.8 %, 18.8 %	10.0 %	19.0 %		
$\varphi(ClNO_2)$	$ClNO_2$ 18.8 %	NO_3^- 10.0 %		21.3 %	This study
	$\gamma(N_2O_5)$	N_2O_5, Cl_2	S_a		
$\varphi(Cl_2)$	34.2 %	18.8 %, 10.4 %	19.0 %	44.6 %	This study
Cl^-, NO_3^-, H_2O				10.0 %	Tham et al. 2016
S_a				19.0 %	Tham et al. 2018

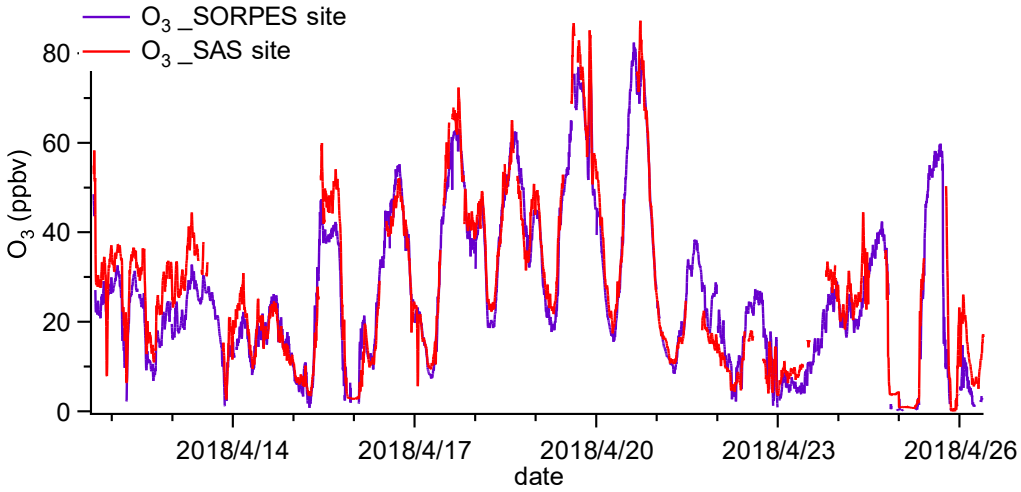

Figure S1. Comparison of O_3 measurements at the SORPES site and the SAS site.

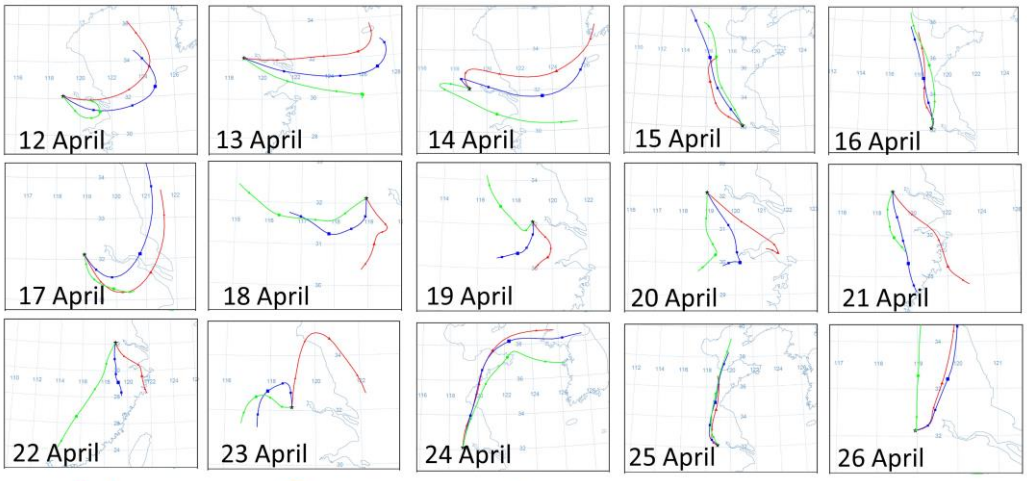

Red: 200m height. Blue: 500 m height. Green: 1000 m height. Local time: 00:00.

Figure S2. Daily backward trajectories arriving at the sampling sites during the field observation period.

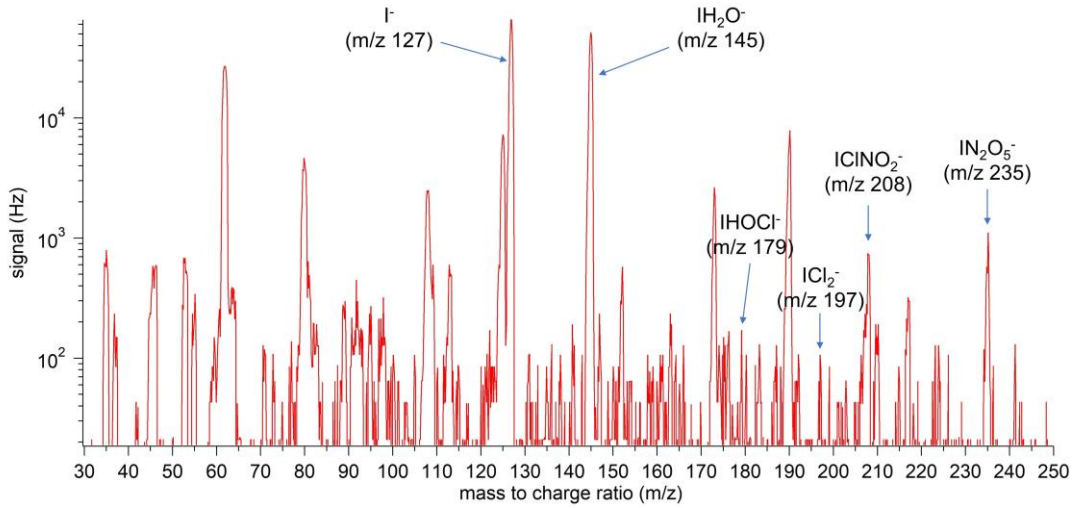

Figure S3. An example of the CIMS spectra taken at 18 April 01:00 LT.

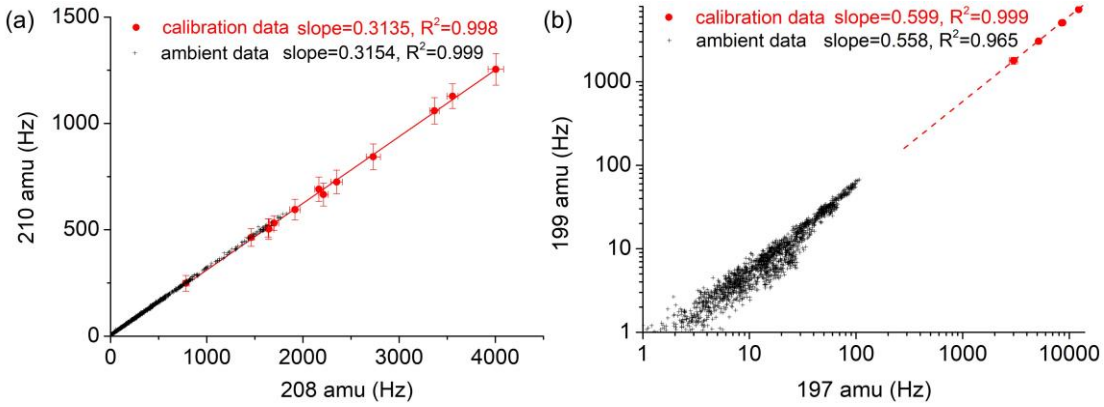

Figure S4. Isotopic analysis of **(a)** $ClNO_2$ and **(b)** Cl_2. The red dots and corresponding fitting lines represent calibration data, while the black crosses "+" denote ambient data.

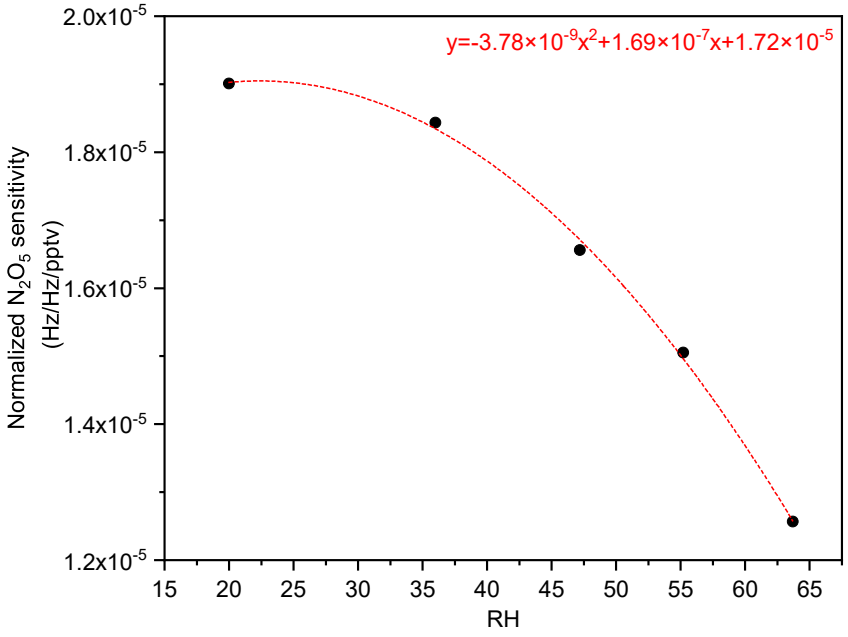

Figure S5. Dependence of the N_2O_5 sensitivity on RH. The normalized sensitivity of N_2O_5 (y axis) was fitted as a quadratic function of RH (x axis), which is $y=-3.78\times10^{-9}x^2+1.69\times10^{-7}x+1.72\times10^{-5}$ ($R^2=1$).

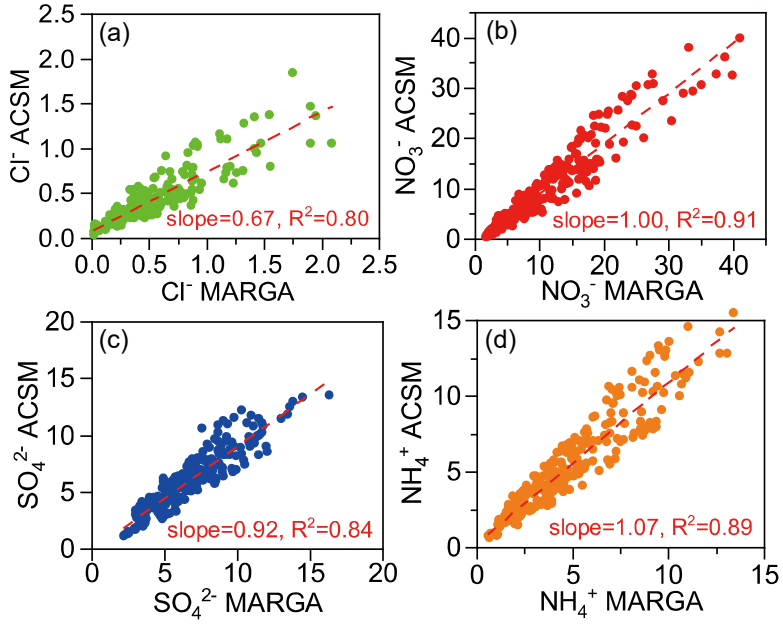

Figure S6. Comparison of ACSM and MARGA data. **(a)**, **(b)**, **(c)**, and **(d)** showed the comparison of Cl^-, NO_3^-, SO_4^{2-}, and NH_4^+ during the whole campaign, respectively. Since the resolution of the MARGA data was 1 hour, the ACSM data was averaged to 1 hour. Units of the ions are all $\mu g/m^3$.

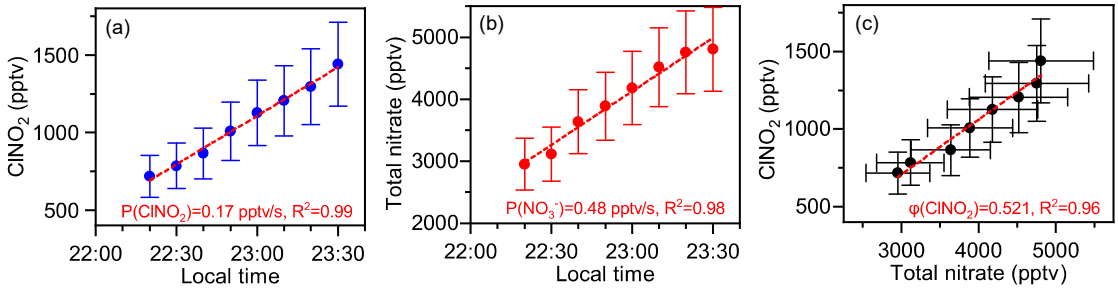

Figure S7. An example showing the calculation of $\gamma(N_2O_5)$ and $\varphi(ClNO_2)$. **(a)** and **(b)** show the increasing rate of $ClNO_2$ and total nitrate observed on the night of Apr 17. **(c)** displays the relationship between $ClNO_2$ and total nitrate shown in **(a)** and **(b)**.

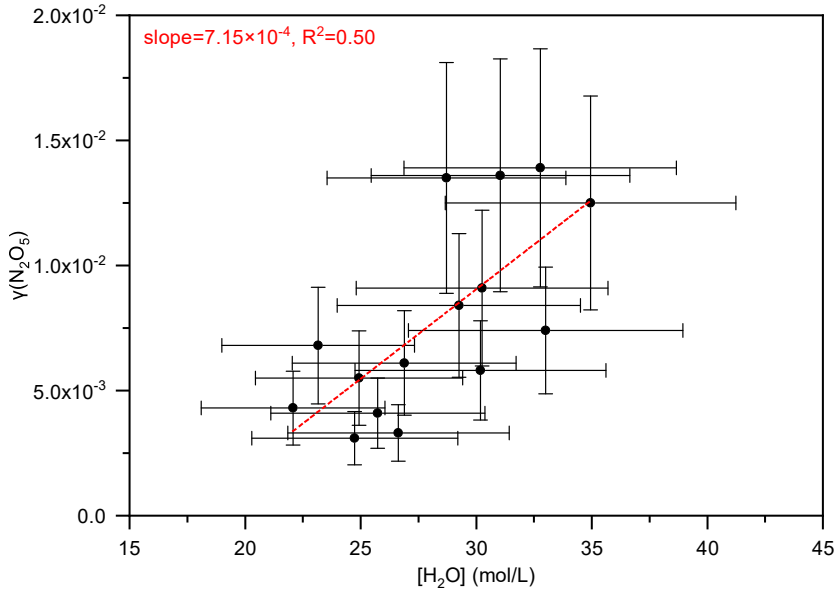

Figure S8. Dependence of $\gamma(N_2O_5)$ on $[H_2O]$.

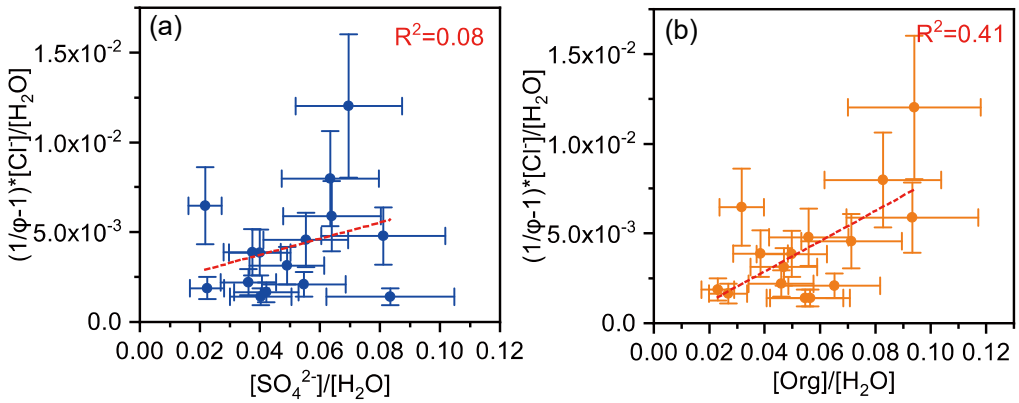

Figure S9. Investigation of the potential of sulfate and total aerosol organics to consume NO_2^+. **(a)** and **(b)** represent sulfate and total organic aerosols, respectively.

References

Kercher, J., Riedel, T., and Thornton, J.: Chlorine activation by N_2O_5: simultaneous, in situ detection of $ClNO_2$ and N_2O_5 by chemical ionization mass spectrometry, Atmospheric Measurement Techniques, 2, 193-204, 2009.

Liao, J., Huey, L. G., Liu, Z., Tanner, D. J., Cantrell, C. A., Orlando, J. J., Flocke, F. M., Shepson, P. B., Weinheimer, A. J., and Hall, S. R.: High levels of molecular chlorine in the Arctic atmosphere, Nature Geoscience, 7, 91, 2014.

Tham, Y. J., Wang, Z., Li, Q., Yun, H., Wang, W., Wang, X., Xue, L., Lu, K., Ma, N., Bohn, B., Li, X., Kecorius, S., Größ, J., Shao, M., Wiedensohler, A., Zhang, Y., and Wang, T.: Significant concentrations of nitryl chloride sustained in the morning: investigations of the causes and impacts on ozone production in a polluted region of northern China, Atmospheric Chemistry

and Physics, 16, 14959-14977, 10.5194/acp-16-14959-2016, 2016.
Tham, Y. J., Wang, Z., Li, Q., Wang, W., Wang, X., Lu, K., Ma, N., Yan, C., Kecorius, S., and Wiedensohler, A.: Heterogeneous N_2O_5 uptake coefficient and production yield of $ClNO_2$ in polluted northern China: Roles of aerosol water content and chemical composition, 2018.